Development 128, 2095-2106 (2001)
Printed in Great Britain © The Company of Biologists Limited 2001
DEV4537

Lung hypoplasia and neonatal death in *Fgf9*-null mice identify this gene as an essential regulator of lung mesenchyme

Jennifer S. Colvin, Andrew C. White, Stephen J. Pratt and David M. Ornitz*

Department of Molecular Biology and Pharmacology, Washington University Medical School, Campus Box 8103, 660 S. Euclid Avenue, St Louis, MO 63110, USA
*Author for correspondence (e-mail: dornitz@pcg.wustl.edu)

Accepted 14 March 2001

SUMMARY

Mammalian lung develops as an evagination of ventral gut endoderm into the underlying mesenchyme. Iterative epithelial branching, regulated by the surrounding mesenchyme, generates an elaborate network of airways from the initial lung bud. Fibroblast growth factors (FGFs) often mediate epithelial-mesenchymal interactions and mesenchymal *Fgf10* is essential for epithelial branching in the developing lung. However, no FGF has been shown to regulate lung mesenchyme. In embryonic lung, *Fgf9* is detected in airway epithelium and visceral pleura at E10.5, but is restricted to the pleura by E12.5. We report that mice homozygous for a targeted disruption of *Fgf9* exhibit lung hypoplasia and early postnatal death. *Fgf9*$^{-/-}$ lungs exhibit reduced mesenchyme and decreased branching of airways, but show significant distal airspace formation and pneumocyte differentiation. Our results suggest that *Fgf9* affects lung size by stimulating mesenchymal proliferation. The reduction in the amount of mesenchyme in *Fgf9*$^{-/-}$ lungs limits expression of mesenchymal *Fgf10*. We suggest a model whereby FGF9 signaling from the epithelium and reciprocal FGF10 signaling from the mesenchyme coordinately regulate epithelial airway branching and organ size during lung embryogenesis.

Key words: FGF9, FGF, FGF receptor, Lung, Mesenchyme, Mouse, Knockout

INTRODUCTION

Chicken lung graft experiments dating back to 1933 demonstrated that mesenchyme is essential for airway branching in embryonic lung. Subsequent studies showed that bronchial mesenchyme stimulates branching, while tracheal mesenchyme inhibits branching (Hilfer, 1996). Recent studies have identified fibroblast growth factor 10 (FGF10) as a mesenchymal signal essential for airway branching (Min et al., 1998; Sekine et al., 1999). We present evidence that an epithelial signal, FGF9, regulates airway branching by stimulating mesenchymal proliferation and modulating *Fgf10* expression.

Lung embryogenesis begins in mice at embryonic day (E)9.5 with the outpocketing of two epithelial buds from the ventral foregut into the surrounding mesoderm. Later lung development is divided into several stages:

(1) During the early pseudoglandular stage (E9.5-E14.2), the lung epithelium branches to form the proximal conducting airways, which are lined by columnar epithelium. At this stage, the epithelial tubes are separated by abundant mesenchyme.

(2) During the late pseudoglandular and canalicular stages (E14.2-E16.6), further airway branching generates bronchial tubules with columnar epithelium, and, distally, acinar tubules with cuboidal epithelium. During this period, the epithelial cells progressively flatten, the proportion of mesenchyme to epithelial tissue decreases, and the terminal buds dilate.

(3) During the saccular stage (E16.6-P5 (postnatal day 5)), distal airspaces form. These airspaces are acinar tubule derivatives, including alveolar ducts, sacs and primitive alveolar structures.

(4) During the alveolar stage (beginning at P5 in mice), alveoli are formed by septation (Bellusci et al., 1997a; Hogan and Yingling, 1998; Quaggin et al., 1999; Ten Have-Opbroek, 1981; Thurlebeck, 1995; Weinstein et al., 1998).

FGF signaling is essential at several stages of mammalian lung development. *Fgf10* and its receptor, *Fgfr2b,* are required for epithelial branching. Targeted deletion of either gene prevents branching, causing the trachea to terminate as a blind sac (De Moerlooze et al., 2000; Min et al., 1998; Sekine et al., 1999). Double *Fgfr3*/*Fgfr4*-null mice survive into adulthood and exhibit normal embryonic lung development, but lack postnatal formation of alveoli (Weinstein et al., 1998). *Fgf7* is expressed in developing lung mesenchyme; but *Fgf7*$^{-/-}$ mice exhibit normal lung morphology, indicating some functional redundancy among Fgf genes in developing lung (Guo et al., 1996). To date, no member of the Fgf family has been demonstrated to regulate lung mesenchyme development.

Fgf9 is one of at least 22 members of the Fgf family (Ornitz and Itoh, 2001). In situ hybridization on mouse embryos detects *Fgf9* expression in skeletal myoblasts, motoneurons, limb apical ectoderm, ventricular myocardium, the mesenteric lining surrounding endoderm-derived organs, gut luminal epithelium and the inner ear (Colvin et al., 1999). At E10.5,

Fgf9 is expressed in the visceral pleura lining the outside of the lung bud and in the epithelium of the developing bronchi. At E12.5 and E14.5 (data not shown), *Fgf9* expression persists in the mesothelium of the visceral pleura, but is no longer detected in airway epithelium (Colvin et al., 1999). This lung expression pattern contrasts with expression of *Fgf10* and *Fgf7*, which are restricted to lung mesenchyme, and suggests novel roles for *Fgf9* in lung development.

To investigate the in vivo functions of *Fgf9*, we generated mice homozygous for a targeted disruption of *Fgf9* (Colvin et al., 2001). Here we report lung hypoplasia and early postnatal death in $Fgf9^{-/-}$ mice. All $Fgf9^{-/-}$ lungs exhibit reduced mesenchyme and decreased airway branching. We further demonstrate that both mesenchymal proliferation and mesenchymal *Fgf10* expression are reduced in $Fgf9^{-/-}$ lung. These findings suggest a model in which epithelial FGF9 and mesenchymal FGF10 coordinately regulate epithelial airway branching and embryonic lung size.

MATERIALS AND METHODS

Gene targeting

The *Fgf9* genomic locus was targeted in SM-1 embryonic stem (ES) cells using a targeting vector engineered to replace 500 bp of the genomic locus with a neomycin resistance cassette. Homologous recombination resulted in a deletion eliminating 224 bp of the 277 bp in the protein-coding region of exon 1 and extending into the first intron (Colvin et al., 2001). Expression from the targeted allele was assessed using RT-PCR of E18.5 brain RNA. The results indicated that no *Fgf9* transcript joining exon 1 to either of the 2 known downstream exons was produced from the mutant allele (Colvin et al., 2001). $Fgf9^{-/-}$ mice were maintained in a mixed 129/C57BL6 background. *Fgf9* genotype was determined by PCR or by Southern blot. Southern blots of *Eco*RI-digested DNA were probed with probe 25.3. The PCR assay produced a 310 bp fragment from the genomic locus and a 234 bp fragment from the targeted allele (Colvin et al., 2001).

Histology

Tissues were fixed in 4% paraformaldehyde or 10% formalin, decalcified if necessary in Surgipath decalcifier II, dehydrated with gradient ethanol, placed in xylene and embedded in paraffin. Sections (5 μm) were cut and stained with Hematoxylin and Eosin. Computer imaging using Foster-Findley PC Image software was used to calculate epithelial and mesenchymal areas on sections of E13.5 lungs. Tissues for plastic sections and transmission electron microscopy were fixed in 2% gluteraldehyde and postfixed in osmium tetroxide before embedding.

Proliferation analysis

$Fgf9^{+/-}$ females that had been mated with $Fgf9^{+/-}$ males were given an intraperitoneal injection of BrdU (120 μg/gram body weight; Sigma) and FrdU (12 μg/gram body weight; Sigma) 1 hour before sacrifice. BrdU antibody staining of lung sections from the resulting embryos was carried out as described (Naski et al., 1998). Sections were counterstained with Methyl Green. Proliferation ratios were determined as BrdU-labeled nuclei over total nuclei in fields viewed through a 20× objective. At E10.5, the 20× field generally includes the entire lung bud. Results were determined to be significant at $P<0.01$.

Lung casts and scanning electron microscopy

Tracheas of E18.5 embryos (or of lungs that had been dissected out of E18.5 embryos) were injected with a 50:1 mixture of Mercox resin and catalyst (Ladd Research Industries, #21245). After allowing the plastic to solidify at room temperature for 1 to 2 hours, lung tissue was removed by immersion in 20% KOH for several days. For s.e.m., plastic casts were dehydrated in graded alcohols, critical-point dried in liquid carbon dioxide, mounted on aluminum stubs and coated with gold (deMello et al., 1997).

Immunohistochemistry

Paraffin sections were rehydrated, trypsin treated (for CCSP and vWF), microwaved (for SP-C and vWF) in antigen unmasking solution (Vector), incubated in methanol/hydrogen peroxide to block endogenous peroxidases and blocked with diluted serum. The primary antibodies used were: an anti-human antiserum against pro-surfactant C (SP-C) (rabbit; a gift from J. Whitsett;1:150 dilution) (Zhou et al., 1996), an anti-mouse CCSP antibody (rabbit; a gift from F. DeMayo;1:2500 dilution) (Ray et al., 1996) and an anti-human vWF antibody (rabbit; from DAKO; 1: 1000 dilution) (Schor et al., 1998). The secondary antibodies used were: a biotinylated goat anti-rabbit IgG (for SP-C and CCSP) and a Cy3-conjugated anti-rabbit IgG (for vWF). For CCSP, the Vectastain ABC-alkaline phosphatase reagent and AP substrate were used (Vector), followed by Eosin counterstaining. For SP-C, the Vectastain ABC-peroxidase reagent and DAB substrate were used (Vector).

Whole-mount in situ hybridization

In situ hybridization was performed as described (Sasaki and Hogan, 1993), with modifications. Control and $Fgf9^{-/-}$ tissues were processed together to ensure identical conditions. Lung tissue was dissected in cold diethyl pyrocarbonate (DEPC) phosphate-buffered saline (PBS), fixed overnight in 4% paraformaldehyde (PFA)/DEPC PBS, dehydrated through graded methanols in DEPC PBT (PBS+0.1% Tween-20) (25%, 50%, 75%, 100%, 100%) and stored at −20°C. For use, tissue was rehydrated and washed with DEPC PBT, digested with proteinase K (10 μg/ml)/DEPC PBT (for 20-25 minutes), rinsed in PBT, fixed in 4% PFA/0.2% glutaraldehyde/DEPC PBT, and rinsed with DEPC PBT. Three-step prehybridization included incubation in (1) 1:1 hybridization solution (50% formamide, 1.3× SSC, 5 mM EDTA, 50 μg/ml yeast tRNA, 0.2% Tween-20, 0.5% Chaps, 100 μg/ml heparin) to PBT mix; (2) hybridization solution; and (3) hybridization solution at 65°C for 1 hour. Tissues were incubated in hybridization solution (~1 μg/ml) for 3 days at 65°C with digoxigenin (DIG)-labeled probes for *Fgf10* (622 bp, provided by B. Hogan) or sonic hedgehog (*Shh*; 642 bp, provided by A. McMahon). Tissue was then washed with 2× SSC w/0.1% Chaps (three times for 20 minutes at 65°C), 0.2× SSC w/0.1% Chaps (three times for 20 minutes at 65°C) and KTBT (50 mM Tris-HCl, 150 mM NaCl, 10 mM KCl, 1% Triton X-100) twice for 5 minutes. Tissue was preblocked with KTBT/20% sheep serum, incubated with anti-DIG Fab alkaline phosphatase conjugate (Boehringer Mannheim) in KTBT/20% sheep serum overnight at 4°C, washed with KTBT (four times for 1 hour), and left overnight in KTBT at 4°C. For the alkaline phosphatase color reaction, tissue was washed with NTMT (40 mM Tris, 100 mM NaCl, 40 mM MgCl, 0.2% Tween-20) twice for 15 minutes, then incubated in the dark with NTMT/BCIP (4.5 μl/ml)/NBT(3 μl/ml). The reaction was stopped by washing in KTBT and post fixing in 4% PFA/PBS for 10 minutes. Stained tissues were dehydrated through graded methanols in PBT and stored at 4°C. For *Fgf10* in situ, $n=3$ at E12.5 and $n=3$ at E13.5-E14.5; for *Shh* in situ, $n=2$.

RESULTS

Neonatal death of $Fgf9^{-/-}$ mice

Mice heterozygous for the targeted allele ($Fgf9^{+/-}$) were phenotypically normal and were bred to produce homozygous

Table 1. *Fgf9*$^{-/-}$ lung weight and bodyweight at E18.5

Genotype	Lung weight (mg±s.d.)*	*P* value‡	Bodyweight (g±s.d.)*	*P* value‡
+/+, +/–	29.6±6.4 (*n*=8§)		1.22±0.08 (*n*=22)	
–/–	8.69±2.1 (*n*=10§)	<0.0001	1.03±0.06 (*n*=6)	<0.0001
% of control	29%		84%	

*Mean lung weight or bodyweight for each group.

‡Two-tail *P* value from two-sample *t*-test assuming equal variances for *Fgf9*$^{-/-}$ lung weight or bodyweight compared with controls.

§*n* refers to the number of lungs weighed. The weight of each lung was determined by averaging three weight measurements.

Table 2. Ratio of mesenchyme to total tissue in *Fgf9*$^{-/-}$ lungs at E13.5

Genotype	*n**	% mesenchyme‡±s.d.	*P* value§
+/+, +/–	18	73.2±4.9	
–/–	18	63.4±6.2	<0.001

**n* refers to the number of 20× fields measured. Sections from three embryos were analyzed for both *Fgf9*$^{-/-}$ and control groups.

‡Mean of mesenchyme tissue areas as percent of the sum of mesenchyme and epithelial tissue areas. Computer imaging using Foster-Findley PC image software was used to calculate tissue areas. Epithelial lumens were included in epithelial areas.

§Two-tail *P* value from two-sample *t*-test assuming equal variances for % mesenchyme in *Fgf9*$^{-/-}$ tissue compared with control tissue.

null mice (*Fgf9*$^{-/-}$). Among 138 heterozygous intercross offspring genotyped at 1 to 3 weeks postpartum, the genotype distribution was: 36%, wild type; 64%, heterozygous; and 0%, null. Newborn pups from heterozygous intercrosses were periodically found dead. All nine of the dead pups yielding usable DNA were *Fgf9*$^{-/-}$. Among an additional 375 embryos harvested at E10.5-E18.5, the genotype distribution was: 24%, wild type; 51%, heterozygous; and 25%, null. These data indicate that *Fgf9*$^{-/-}$ mice survive embryonic development but die in the early postnatal period.

Definitive pathology in *Fgf9*$^{-/-}$ mice has been observed in the lung and reproductive system. *Fgf9*$^{-/-}$ mice exhibit dramatic lung hypoplasia. Male-to-female sex reversal in *Fgf9*$^{-/-}$ mice is described elsewhere (Colvin et al., 2001). Total mean bodyweight of E18.5 *Fgf9*$^{-/-}$ mice was 84% of that of controls (Table 1). The etiology of embryonic growth retardation is unclear. Variable dilation of cardiac atria and ventricles was observed in E14.5-E18.5 *Fgf9*$^{-/-}$ embryos, suggesting possible cardiovascular insufficiency. *Fgf9* is expressed in E10.5-E12.5 heart in the region of the developing interventricular septum (Colvin et al., 1999), suggesting a possible role for *Fgf9* in cardiac development. However, similar variable cardiac chamber dilation in *Fgf10*$^{-/-}$ embryos (J. S. C., unpublished), which lack lungs (Min et al., 1998; Sekine et al., 1999), suggests that cardiac dilation in *Fgf9*$^{-/-}$ mice may be secondary to lung hypoplasia.

Fgf9$^{-/-}$ mice die shortly after birth, apparently owing to hypoxia. Among eight E18.5 *Fgf9*$^{-/-}$ pups observed after Caesarian section, all pups moved, seven out of eight breathed and several became somewhat pink. By 30 minutes postpartum, all seven breathing pups exhibited agonal breathing and cyanosis. One naturally delivered *Fgf9*$^{-/-}$ pup remained pink and active until sacrificed about 20 minutes postpartum. Thus, E18.5 *Fgf9*$^{-/-}$ pups can breathe, and (initially) some ventilate enough to become pink, indicating oxygenation of systemic tissues; however, they become severely cyanotic shortly thereafter. About 40% of *Fgf9*$^{-/-}$ embryos exhibit cleft palate (A. C. W., unpublished). Cyanosis and neonatal death are associated with cleft palate in *Tgfb3*$^{-/-}$ and *Msx1*$^{-/-}$ (Satokata and Maas, 1994) mice, suggesting that cleft palate may contribute to the death of some *Fgf9*$^{-/-}$ mice. However, *Tgfb3*$^{-/-}$ mice die at 11-20 hours after birth (Kaartinen et al., 1995), a less precipitous decline than observed in *Fgf9*$^{-/-}$ mice. These findings suggest that hypoxia secondary to lung hypoplasia causes the neonatal death of *Fgf9*$^{-/-}$ mice.

Lung hypoplasia in *Fgf9*$^{-/-}$ mice

The lung hypoplasia phenotype is 100% penetrant with little variation in severity. All *Fgf9*$^{-/-}$ E12.5-E18.5 lungs examined were hypoplastic (*n*=48). Mean wet weight of E18.5 *Fgf9*$^{-/-}$ lungs was 29% that of controls, whereas mean *Fgf9*$^{-/-}$ total body weight was 84% that of controls (Table 1). Hence, generalized reduction in embryonic growth cannot account for the decreased lung volume in *Fgf9*$^{-/-}$ mice. The number and orientation of lobes is preserved in *Fgf9*$^{-/-}$ lungs (Fig. 1A,B), indicating that very early epithelial branching occurs normally. Primary bronchi in E12.5-13.5 *Fgf9*-/- lungs were as long as those of controls (data not shown), indicating that longitudinal growth of airways is at least initially preserved. However, in contrast to those of littermate controls, E14.5 *Fgf9*$^{-/-}$ lungs failed to fill the thoracic cavity (Fig. 1C,D). The diaphragm in *Fgf9*$^{-/-}$ mice was intact (Fig. 1D), and no abdominal organs were observed in the thoracic cavity of *Fgf9*$^{-/-}$ mice. These findings suggest that a primary defect in lung growth, rather than compression of the developing lung, causes *Fgf9*$^{-/-}$ lung hypoplasia.

Mesenchymal hypoplasia in *Fgf9*$^{-/-}$ lungs

To investigate the origin of the lung hypoplasia phenotype, we examined *Fgf9*$^{-/-}$ lungs starting at E10.5, shortly after initial formation of the bronchial buds. E10.5 and most E11.5 *Fgf9*$^{-/-}$ lungs were grossly and histologically indistinguishable from controls (Fig. 1I,J). By E12.5, lung and mesenchymal tissue hypoplasia were apparent on gross examination of *Fgf9*$^{-/-}$ lungs (Fig. 1E,F). Histology (Fig. 1K,L) and quantitative analysis of tissue areas (Table 2) revealed a reduced ratio of mesenchyme to epithelial tissue in E13.5 *Fgf9*$^{-/-}$ lungs relative to controls. All E12.5-E14.5 *Fgf9*$^{-/-}$ lungs grossly or histologically examined showed lung hypoplasia and reduced lung mesenchyme (*n*=19). By E12.5, some peripheral epithelial buds in *Fgf9*$^{-/-}$ lungs appeared to be dilating, a process that normally coincides with the thinning of mesenchyme and distal epithelial differentiation later in lung development (Fig. 1G,H; Bellusci et al., 1997a; Ten Have-Opbroek, 1981). This observation suggests that the reduction in the amount of mesenchyme in *Fgf9*$^{-/-}$ lungs may allow premature dilation of epithelial buds.

Epithelial and mesenchymal proliferation in lung tissue was assessed by BrdU immunohistochemistry after a 1 hour exposure to BrdU in utero (Table 3). Mesenchymal proliferation was significantly reduced in *Fgf9*$^{-/-}$ lungs relative to controls at E10.5-E11.5. No difference in epithelial

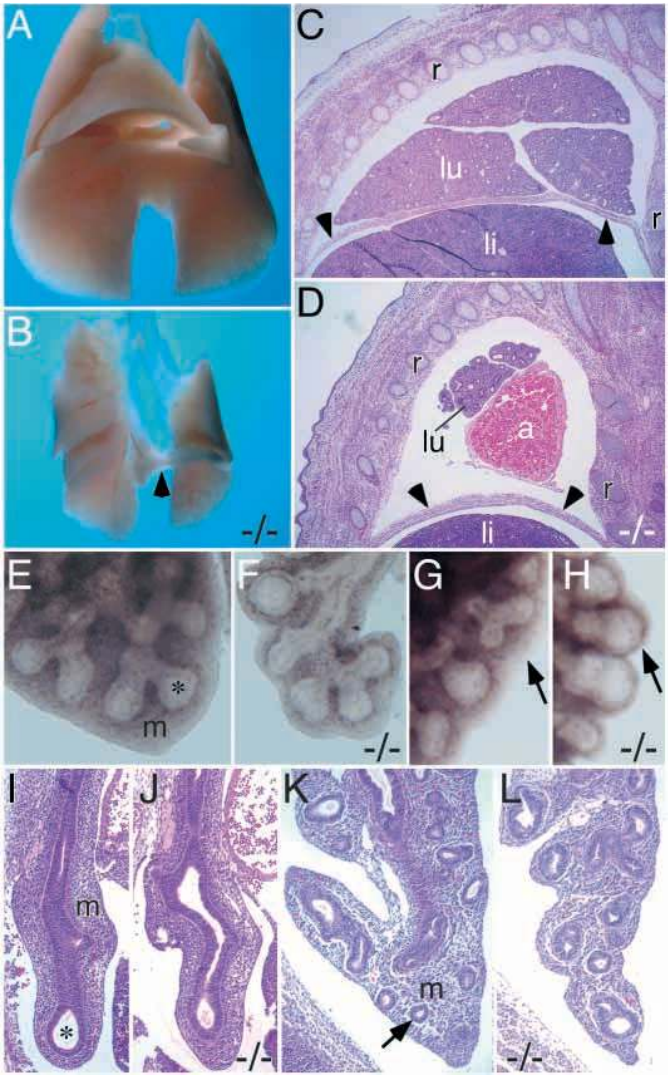

Fig. 1. Morphological and histological analysis of *Fgf9*$^{-/-}$ lungs. (A,B) Anterior views of gross dissections of uninflated control (A) and *Fgf9*$^{-/-}$ (B) lungs at E18.5. The *Fgf9*$^{-/-}$ lung is smaller but contains the same lobes as the control. Arrowhead in B indicates the accessory lobe. (C,D) Sagittal sections of the right side of the thoracic cavity at similar levels from E14.5 control (C) and *Fgf9*$^{-/-}$ (D) embryos. The control lung (lu) fills the thoracic cavity while the *Fgf9*$^{-/-}$ lung does not. A dilated cardiac atrium (a) is observed adjacent to the *Fgf9*$^{-/-}$ lung (D). An intact diaphragm (arrowheads) is seen just superior to the liver (li) in both C,D. (E,F) High power views of the caudal part of the right lower lobe of grossly dissected E12.5 control (E) and *Fgf9*$^{-/-}$ (F) lungs. Note the lack of mesenchyme and the reduced branching complexity in the *Fgf9*$^{-/-}$ lung relative to the control. (G,H) High-power views of the left lobe of grossly dissected E12.5 control (G) and *Fgf9*$^{-/-}$ (H) lungs. Epithelial buds in the *Fgf9*$^{-/-}$ lung (arrow in H) appear dilated and have less adjacent mesenchyme than comparably located epithelial buds in the control lung (arrow in G). In addition, a control lung bud (arrow in G) is branching into two buds, while the corresponding *Fgf9*$^{-/-}$ bud (arrow in H) is not branching. (I,J) Sagittal sections of E11.5 lungs showing similar appearance of control (I) and *Fgf9*$^{-/-}$ (J) samples. (K,L) E13.5 lung sections showing reduced mesenchyme in *Fgf9*$^{-/-}$ (L) compared with control lung (K). Small diameter airways are more prevalent in control lung (arrow in K) than in *Fgf9*$^{-/-}$ lung. (I-L) are shown at the same magnification. m, mesenchyme; r, ribs; asterisks indicate future airspaces within epithelial branches.

Table 3. Cell proliferation in *Fgf9*$^{-/-}$ lungs

Age	Genotype	*n**	Tissue	% labeled‡ ±s.d.	*P* value§
E10.5-E11.5	+/+, +/–	16	Epithelium	58.7±8.7	
	–/–	18	Epithelium	56.0±8.0	0.34
	+/+, +/–	16	Mesenchyme	59.6±4.6	
	–/–	18	Mesenchyme	50.7±7.7	<0.01
E13.5	+/+, +/–	23	Epithelium	59.0±5.9	
	–/–	22	Epithelium	57.6±6.6	0.48
	+/+, +/–	23	Mesenchyme	51.7±6.5	
	–/–	22	Mesenchyme	53.2±6.1	0.43

**n* refers to number of 20× fields of view counted. At E10.5-E11.5, sections from five *Fgf9*$^{-/-}$ embryos and six control embryos were used. At E13.5, sections from two *Fgf9*$^{-/-}$ embryos and two control embryos were used.

‡Lung sections from BrdU-exposed embryos were stained using anti-BrdU antibody and counterstained with Methyl Green. Embryos were harvested 1 hour after intraperitoneal BrdU injection of pregnant females. % labeled refers to the number of BrdU labeled cells/total cells and represents the % of proliferating cells within the epithelium or mesenchyme. The ratios of total epithelial cells counted/total mesenchymal cells counted for each group are as follows: (2904/9232) for E10.5-E11.5 control; (3588/8000) for E10.5-E11.5 *Fgf9*$^{-/-}$; (7495/18498) for E13.5 control; and (7136/13457) for E13.5 *Fgf9*$^{-/-}$.

§Two-tail *P* value from two-sample *t*-test assuming equal variances for % labeled cells in *Fgf9*$^{-/-}$ tissue compared with control tissue.

proliferation between *Fgf9*$^{-/-}$ lungs and controls was observed at E10.5-E11.5. At E13.5, no difference in mesenchymal or epithelial proliferation between *Fgf9*$^{-/-}$ lungs and controls was detected. This suggests that FGF9 drives mesenchymal proliferation primarily early in lung development, when *Fgf9* is expressed in both the epithelium and the pleura. Although equal proportions of mesenchymal cells are proliferating in control and *Fgf9*$^{-/-}$ lungs at E13.5, there are fewer total mesenchymal cells in E13.5 *Fgf9*$^{-/-}$ lungs than in controls. Hence, the normal decline in mesenchymal thickness as lung development progresses would be expected to occur prematurely in *Fgf9*$^{-/-}$ lungs.

Reduced airway branching in *Fgf9*$^{-/-}$ lungs

During early embryonic development, extensive branching of epithelial buds (about 16 generations in humans) generates conducting airways (Fig. 2J). Conducting airways are lined with columnar epithelium and function after birth, in part, to transport air in and out of the lung. Later iterations of epithelial branching (generations 17-23 in humans) generate respiratory airways, which function after birth to exchange oxygen and carbon dioxide between air and blood (Hasleton, 1996a). Walls of respiratory airways contain small alveolar sacs, which are further subdivided into alveoli by postnatal septation. *Fgf9*$^{-/-}$ lung hypoplasia could be the result of (1) decreased branching of airways and/or (2) failure of development of distal lung respiratory structures, including the alveolar ducts and sacs.

Histological and morphological examination was used to assess airway branching in *Fgf9*$^{-/-}$ lungs. Preservation of number and orientation of lobes in *Fgf9*$^{-/-}$ lungs suggests that the earliest stages of proximal branching are preserved (Fig. 1A,B). By E12.5, however, epithelial branching was less extensive in *Fgf9*$^{-/-}$ lungs than in controls (Fig. 1E,F). The observation that lung hypoplasia and reduced epithelial complexity in *Fgf9*$^{-/-}$ lungs is well established by E12.5, prior to the onset of distal airspace formation, suggests that

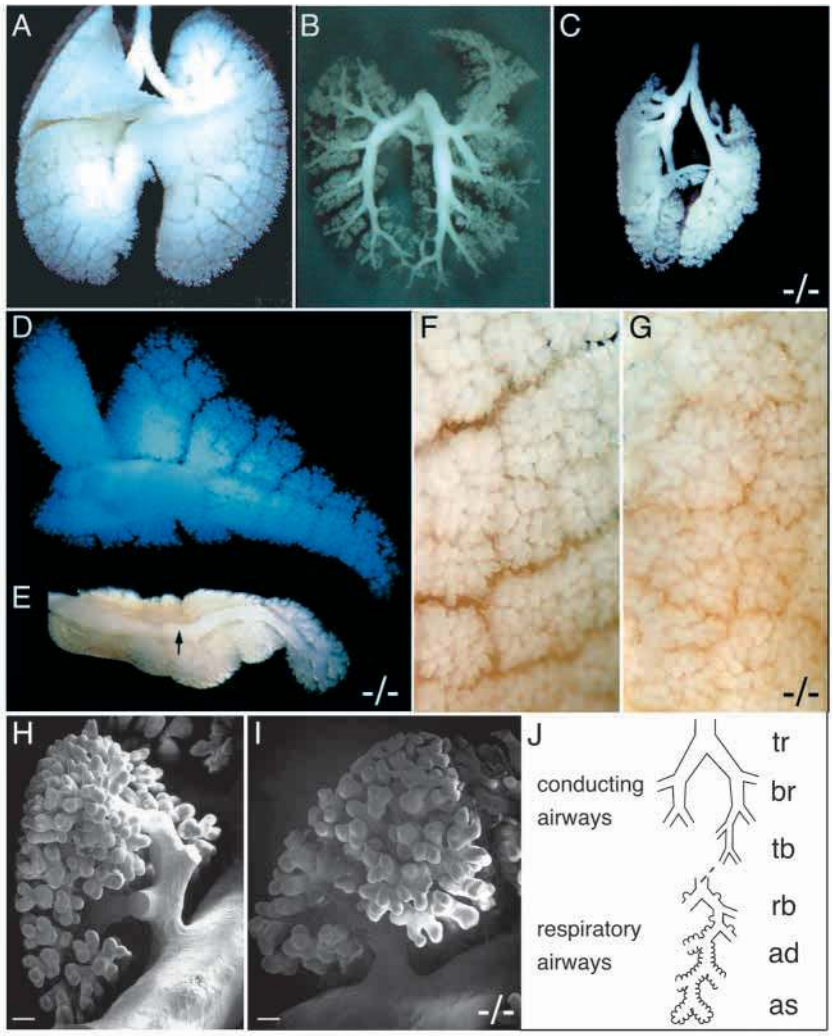

Fig. 2. Analysis of airway branching in E18.5 *Fgf9*$^{-/-}$ lungs using epithelial casts. (A-C) Epithelial casts of whole control (A) and *Fgf9*$^{-/-}$ (C) lungs. The *Fgf9*$^{-/-}$ lung cast is smaller than the control but exhibits evidence of both proximal airway branching and distal airspace formation. Some proximal branches are observed in the upper part of the *Fgf9*$^{-/-}$ cast, and alveolar sacs covering the surface indicate generation of distal airways. (B) An underinjected epithelial cast of a control lung showing a network of proximal branches that is larger than the total size of the *Fgf9*$^{-/-}$ cast (C). (D,E) Accessory lobe casts dissected from whole lung epithelial casts of control (D) and *Fgf9*$^{-/-}$ (E) lungs. (E is shown at 1.2× the magnification of D.) The lung cast shown in (E) was overinjected to ensure filling of all airway branches. Note the absence of branches along much of the *Fgf9*$^{-/-}$ accessory lobe bronchus (arrow), while further iterations of branches obscure the main bronchus of the control accessory lobe. (F,G) High-power views of the dorsal side of the left lobe of control (F) and *Fgf9*$^{-/-}$ (G) lung casts showing a similar density of alveolar sacs on the lung surface. (H,I) Scanning electron microscope images of control (H) and *Fgf9*$^{-/-}$ (I) lung casts, showing similar structure of distal clusters of alveolar sacs. The normal structure of dense tufts of alveolar sacs in (I), and the normal density of surface alveolar sacs in (G), together suggest that significant distal airspace formation occurs in *Fgf9*$^{-/-}$ lung. (J) Schematic diagram of the progression of epithelial airways from proximal conducting airways to distal respiratory airways in embryonic lung. Respiratory airways are distinguished from conducting airways by the presence of alveolar sacs in the walls of respiratory airways. (Respiratory bronchioles (rb), which serve as both conducting and respiratory airways in humans and in many animals, are not found in rodents.) Alveoli are formed by septation of alveolar sacs, a process that occurs in mice only after birth. Scale bars: 50 μm in H,I. ad, alveolar duct; as, alveolar sac; br, bronchus; rb, respiratory bronchiole; tb, terminal bronchiole; tr, trachea.

reduced proximal airway branching contributes significantly to *Fgf9*$^{-/-}$ lung pathology. At E13.5, secondary branching of the accessory lobe had occurred in control lungs but was absent from *Fgf9*$^{-/-}$ lungs (data not shown). Although peripheral epithelial buds in E12.5-E13.5 control lungs were readily observed in the process of budding into two epithelial branches (arrow in Fig. 1G), peripheral buds in *Fgf9*$^{-/-}$ lungs generally appeared dilated and unbranched (Fig. 1H). Sections of *Fgf9*$^{-/-}$ lungs at E13.5 (Fig. 1L) and E14.5 (data not shown) showed fewer small diameter airways than controls (arrow in Fig. 1K), also suggesting reduced airway branching. In sections of E18.5 lungs, fewer generations of conducting airways were seen in *Fgf9*$^{-/-}$ lungs than in controls (see Fig. 4A,B below). These results indicate impaired airway branching in *Fgf9*$^{-/-}$ lungs.

To assess further whether decreased airway branching and/or distal airspace formation contributed to lung hypoplasia in *Fgf9*$^{-/-}$ mice, we studied airway branching using plastic epithelial casts of E18.5 lungs. All *Fgf9*$^{-/-}$ lung casts generated (n=15) were smaller than controls, but exhibited evidence of both proximal branching and distal airspace formation (Fig. 2A-C). Proximal branching can be observed in underinjected casts, generated by injecting less plastic than is required to expand the lungs fully. Underinjected control casts exhibited an extensive network of proximal branches (Fig. 2B). The scaffolding of proximal branches in control casts was larger than the total size of more fully injected *Fgf9*$^{-/-}$ casts (Fig. 2C). The main bronchus of the accessory lobe in control casts is hidden by an extensive network of airway branching (Fig. 2D). In contrast, the main bronchus of the accessory lobe is readily visible in *Fgf9*$^{-/-}$ lung casts. Even in overinjected *Fgf9*$^{-/-}$ casts, much of the main bronchus of the accessory lobes lacked secondary branching (arrow in Fig. 2E). These findings further demonstrate impaired airway branching in *Fgf9*$^{-/-}$ lungs.

Epithelial lung casts also allowed us to assess distal airspace development. Outer surfaces of control (Fig. 2A,F) and *Fgf9*$^{-/-}$ (Fig. 2C,G) lung casts showed comparable density of alveolar sacs, indicating that alveolar sac formation can occur in the absence of *Fgf9*. Scanning electron microscopy of lung casts showed similar structure of distal alveolar sac clusters in control (Fig. 2H) and *Fgf9*$^{-/-}$ (Fig. 2I) casts. This indicates that development of several generations of distal respiratory airways can occur without *Fgf9*. Normal density of air sacs on the lung surface and normal structure of distal airway clusters,

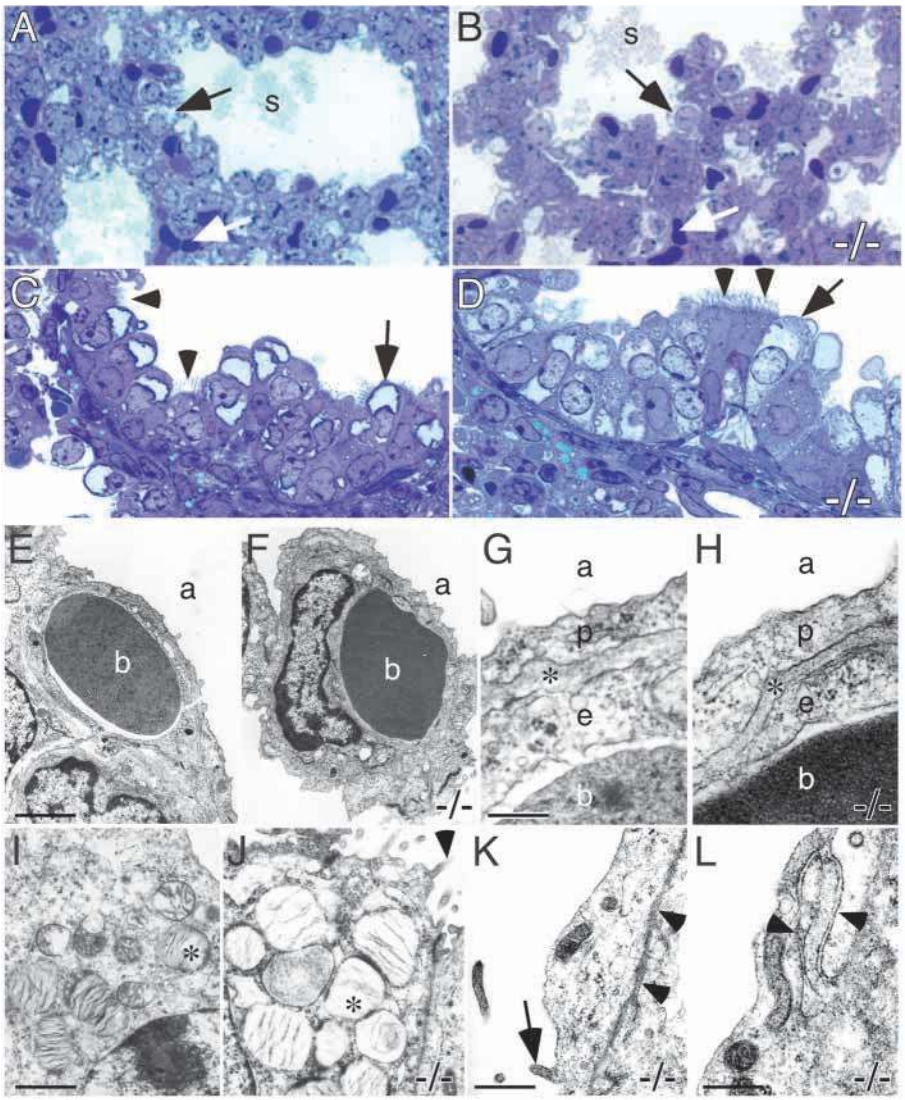

Fig. 3. Normal distal and proximal differentiation in E18.5 *Fgf9*$^{-/-}$ lungs. (A-D) Toluidine Blue stained plastic sections of control (A,C) and *Fgf9*$^{-/-}$ (B,D) lungs showing normal differentiation of distal (A,B) and proximal (C,D) epithelium. (A,B) Sections of control (A) and *Fgf9*$^{-/-}$ (B) distal lung showing similar epithelial structure between alveolar sac airspaces. Surfactant (s) is seen in airways in A,B. Note that capillaries (white arrows) are present and similarly located within surrounding tissue in A,B. Differentiating epithelial cells display characteristic vacuolization due to loss of glycogen during section processing (black arrows in A,B). (C,D) Sections of proximal airway in control (C) and *Fgf9*$^{-/-}$ (D) lungs show similar epithelial architecture. Normal appearing ciliated cells (arrowheads) and Clara cells (arrows) are seen in control (C) and *Fgf9*$^{-/-}$ (D) sections. (E-L) Transmission electron micrographs of E18.5 control and *Fgf9*$^{-/-}$ lungs. (E,F) Control (E) and *Fgf9*$^{-/-}$ (F) lung capillaries showing the gas diffusion barrier between airspace (a) and blood (b). (G,H) Higher power views of the diffusion barrier in control (G) and *Fgf9*$^{-/-}$ (H) lungs, demonstrating normal close apposition of endothelial cell processes (e) and Type I pneumocyte processes (p), separated by basement membrane (asterisks). (I) A Type II pneumocyte from a control lung showing lamellar bodies (asterisk). (J) A Type II pneumocyte from an *Fgf9*$^{-/-}$ lung showing lamellar bodies (asterisk) and surface microvilli (arrowhead). (K) Transmission electron microscopy of the surface of an *Fgf9*$^{-/-}$ lung showing the basement membrane (arrowheads) beneath and a long microvillus (arrow) on the surface of a pleural mesothelial cell. (L) Transmission electron micrograph of the surface of an *Fgf9*$^{-/-}$ lung showing a tight junction (arrowheads) between two pleural mesothelial cells. (The tight junction is the extended s-shaped region of close apposition between the plasma membranes of neighboring pleural cells.) Scale bars: 1.1 μm in E,F; 0.15 μm in G,H; 0.5 μm in I,J; 0.28 μm in K; 0.22 μm in L.

together indicate preservation of significant distal airway development in *Fgf9*$^{-/-}$ lung. In contrast, *Pod1*$^{-/-}$ mice (*Tcf21* – Mouse Genome Informatics), which show moderately reduced proximal airway branching, exhibit nearly complete absence of distal airspace formation (Quaggin et al., 1999). *Fgf9*$^{-/-}$ lungs clearly have fewer alveolar sacs overall than controls (Fig. 2A,C). This could result from either impaired branching of proximal airways, or from generalized impairment of both proximal branching and distal airspace formation.

Normal proximal and distal cellular morphology in *Fgf9*$^{-/-}$ lungs

To carry out gas exchange after birth, the distal lung must undergo extensive morphological changes late in fetal development. These changes include thinning of the epithelium, differentiation of pneumocytes, development of capillaries and close juxtaposition of capillaries to flattened pneumocytes that line the walls of alveolar sacs. Gas exchanged between blood in the capillaries and air in the alveolar sacs must diffuse across the three layers of the alveolar sac wall (i.e. the squamous Type I pneumocyte, the intervening basement membrane and the capillary endothelial cell). Pneumocytes in alveolar sac walls must be thin and closely associated with thin capillary endothelial cells to allow efficient diffusion.

To assess distal differentiation, we analyzed E18.5 *Fgf9*$^{-/-}$ lungs using plastic-embedded sections and transmission electron microscopy. Similar distal architecture was observed in *Fgf9*$^{-/-}$ and control lungs (Fig. 3A,B). Abundant capillaries and close apposition of capillaries to alveolar spaces were seen in both *Fgf9*$^{-/-}$ and control lungs (Fig. 3A,B), as was normal air:blood diffusion barrier morphology (Fig. 3E-H). Transmission electron microscopy revealed lamellar bodies within Type II pneumocytes in control and *Fgf9*$^{-/-}$ lungs (Fig. 3I,J). Type II cells in *Fgf9*$^{-/-}$ lungs also exhibited characteristic surface microvilli (arrowhead in Fig. 3J). These results indicate that distal lung differentiation is preserved in *Fgf9*$^{-/-}$ mice.

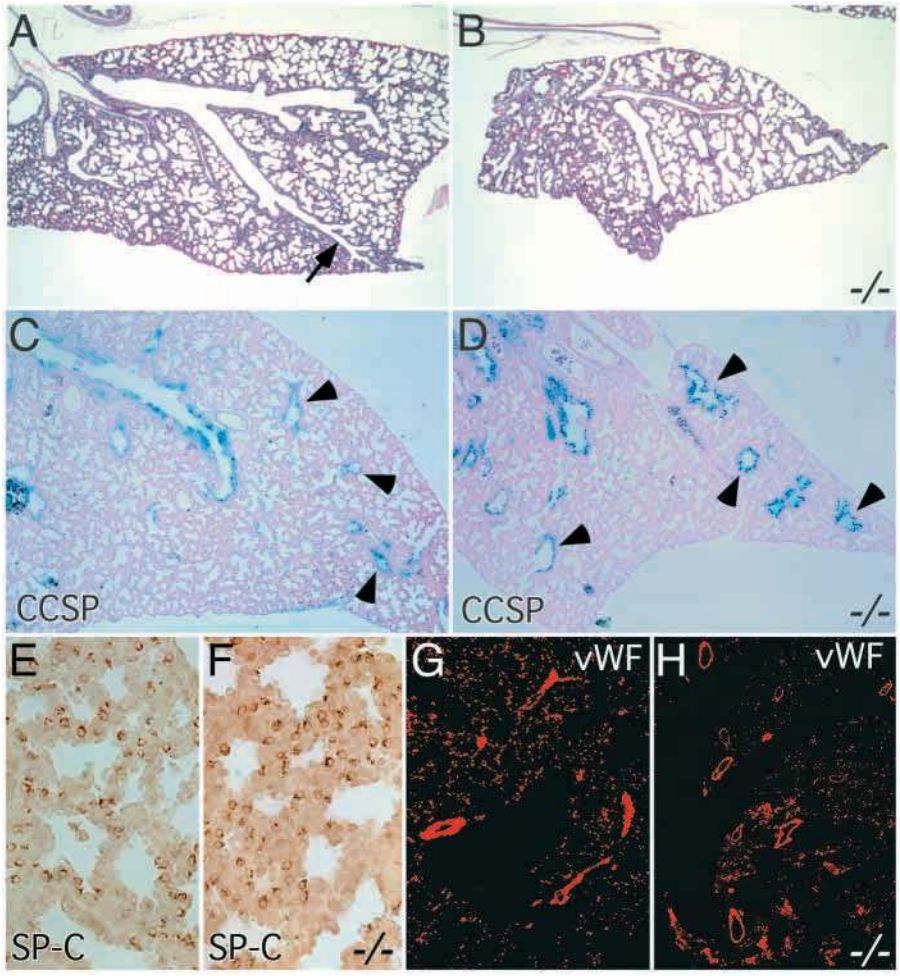

Fig. 4. Immunohistochemistry for epithelial and vascular markers in E18.5 *Fgf9*$^{-/-}$ lungs. (A,B) Hematoxylin and Eosin stained sections of the left lobe of control (A) and *Fgf9*$^{-/-}$ (B) lungs. Note that fewer generations of conducting airways (i.e. airways without alveolar sacs in their walls) are seen in the *Fgf9*$^{-/-}$ lungs compared with controls. (The arrow in A indicates a conducting airway.) Distal aspects of both lungs have similar alveolar duct and alveolar sac structures, which are particularly evident in the less expanded upper regions of the lung sections (leftmost regions of (A,B)). (C,D) Immunohistochemistry for CCSP in lung sections from control (C) and *Fgf9*$^{-/-}$ (D) embryos. *Fgf9*$^{-/-}$ lung (D) shows normal expression of CCSP in Clara cells in proximal airways. Note the relatively larger diameter of CCSP-positive airways (arrowheads) in *Fgf9*$^{-/-}$ versus control lung, indicating reduced branching of conducting airways. (E,F) Immunohistochemistry for SP-C in lung sections from control (E) and *Fgf9*$^{-/-}$ (F) embryos. *Fgf9*$^{-/-}$ lung (F) shows expression of surfactant in Type II pneumocyte cytoplasm that is comparable with that in the control (E). (G,H) Immunohistochemistry for vWF in lung sections from control (G) and *Fgf9*$^{-/-}$ (H) embryos, showing normal staining of large vessels in *Fgf9*$^{-/-}$ lung.

Fgf9 is expressed in the developing visceral pleura (Colvin et al., 1999). However, pleural structure, including surface microvilli on pleural mesothelial cells, tight junctions between pleural cells, and the underlying basement membrane, appears to be preserved in *Fgf9*$^{-/-}$ lungs (Fig. 3K,L).

Finally, sections of proximal airways at E18.5 indicate normal cellular differentiation and epithelial organization in *Fgf9*$^{-/-}$ lungs (Fig. 3C,D). Proximal epithelium includes both ciliated cells and Clara cells. Clara cells are nonciliated secretory cells found mainly in terminal and respiratory bronchioles (Hasleton, 1996a). Both control and *Fgf9*$^{-/-}$ lung sections exhibited histologically normal cilated cells (arrowheads in Fig. 3C,D) and Clara cells (arrows in Fig. 3C,D).

Normal expression of proximal and distal markers in *Fgf9*$^{-/-}$ lungs

Sections of E18.5 control (Fig. 4A) and *Fgf9*$^{-/-}$ lungs (Fig. 4B) both show large proximal epithelial branches, but control lung sections show more smaller diameter conducting airways (arrow in Fig. 4A) than do *Fgf9*$^{-/-}$ sections. Control and *Fgf9*$^{-/-}$ lungs exhibit similar distal epithelial structures, including alveolar ducts and sacs, which are particularly evident in the less expanded upper regions of the lung (leftmost regions of Fig. 4A,B). To evaluate epithelial cell differentiation in E18.5 lung, we analyzed expression of proximal and distal lung epithelial cell markers using immunohistochemistry. Clara cell secretory protein (CCSP) is produced by Clara cells in the proximal lung epithelium. Staining with CCSP antibody revealed CCSP expression in Clara cells in E18.5 control (Fig. 4C) and *Fgf9*$^{-/-}$ (Fig. 4D) lungs. Surfactant C (SP-C) is expressed in Type II pneumocytes in distal lung epithelium (Wert et al., 1993). Sections from E18.5 control (Fig. 4E) and *Fgf9*$^{-/-}$ (Fig. 4F) lungs showed normal expression of SP-C in Type II pneumocyte cytoplasm. Extensive expression of CCSP and SP-C indicates that normal differentiation of Clara cells and Type II pneumocytes, respectively, can occur in the absence of *Fgf9*.

The CCSP staining pattern indicates a lack of small diameter conducting airways in *Fgf9*$^{-/-}$ lung. The diameter of the most distal CCSP positive airways (arrowheads in Fig. 4C,D) is larger in *Fgf9*$^{-/-}$ sections than in controls. Because CCSP is expressed in proximal airways, and airway diameter decreases as branching progresses, this indicates that branching of proximal airways is reduced in *Fgf9*$^{-/-}$ lung. As CCSP is expressed primarily in the distalmost conducting airways (i.e. the terminal and respiratory bronchioles), this observation suggests that branching of the smaller conducting airways is regulated by *Fgf9*.

To assess vascular differentiation in *Fgf9*$^{-/-}$ lungs, we used immunohistochemistry to analyze vonWillebrand Factor (vWF) expression in E18.5 lung. vWF antibody selectively

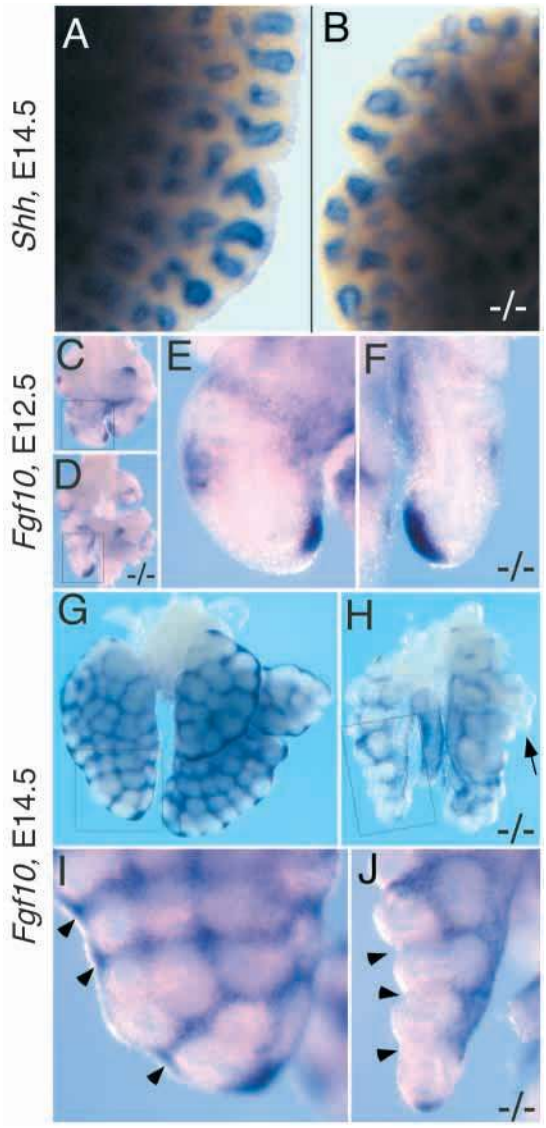

Fig. 5. Whole-mount in situ hybridization for *Shh* and *Fgf10* in embryonic *Fgf9*$^{-/-}$ lungs. (A,B) In situ hybridization for *Shh* in E14.5 control (A) and *Fgf9*$^{-/-}$ (B) lungs. Epithelial *Shh* expression in *Fgf9*$^{-/-}$ lung is comparable with that in control lungs. (C-F) *Fgf10* expression in E12.5 control (C,E) and *Fgf9*$^{-/-}$ (D,F) lungs. (E,F) Higher magnification images of the boxed regions in C,D, respectively. Note comparable expression of *Fgf10* in mesenchyme distal to airway buds in control (C,E) and *Fgf9*$^{-/-}$ (D,F) lungs. (G-J) *Fgf10* expression in E14.5 control (G,I) and *Fgf9*$^{-/-}$ (H,J) lungs. *Fgf9*$^{-/-}$ lung (H) shows reduced expression of *Fgf10* relative to control lung (G). Note the absence of *Fgf10* expression in the region of H indicated by the arrow and the presence of *Fgf10* expression in the corresponding region of G. The indicated *Fgf10* negative buds (arrow in H) are dilated with little surrounding mesenchyme (similar to buds in Fig. 2J); this suggests that absence of *Fgf10* expression may be due to a lack of mesenchymal tissue. (H is shown at 1.4× the magnification of G.) (I,J) Higher magnification images of the boxed regions of G,H, respectively. Note control *Fgf10* expression in the mesenchyme between epithelial buds (arrowheads in I). No *Fgf10* expression is seen in the comparable regions of the *Fgf9*$^{-/-}$ lung (arrowheads in J). (I,J are at the same magnification.)

stains large to medium sized arteries and veins (Kuzu et al., 1992). Expression of vWF in large blood vessels was comparable in control and *Fgf9*$^{-/-}$ lungs (Fig. 4G,H). Plastic sections and transmission electron microscopy both showed normal capillary distribution and morphology in *Fgf9*$^{-/-}$ lung (Fig. 3B,F). Finally, Hematoxylin and Eosin stained sections of *Fgf9*$^{-/-}$ lungs exhibited normal histology and distribution of blood vessels (data not shown). These findings suggest that development of lung vasculature can occur in the absence of *Fgf9*. Hence, loss of blood supply secondary to reduced mesenchyme is unlikely to account for *Fgf9*$^{-/-}$ lung hypoplasia.

Shh and *Fgf10* expression in *Fgf9*$^{-/-}$ lungs

Fgf10 and *Shh* are both essential for lung embryogenesis: *Fgf10*$^{-/-}$ mice lack lungs (Min et al., 1998; Sekine et al., 1999) and *Shh*$^{-/-}$ mice have dysmorphic lungs (Pepicelli et al., 1998). To determine whether aberrant expression of *Shh* and/or *Fgf10* contributes to the *Fgf9*$^{-/-}$ lung phenotype, we used whole-mount in situ hybridization to assess expression of *Shh* and *Fgf10* in embryonic *Fgf9*$^{-/-}$ lungs. *Shh* is expressed in the epithelium of developing mouse lung from E11.5 through E18.5 (Bellusci et al., 1997a). E14.5 control (Fig. 5A) and *Fgf9*$^{-/-}$ (Fig. 5B) lungs showed comparable epithelial *Shh* expression.

During early lung embryogenesis, *Fgf10* is detected in foci of high expression in lung mesenchyme distal or adjacent to budding airway epithelium. *Fgf10* expression is observed in mesenchyme at the distal tip of the prospective lobes starting at about E10.0. By E12.5, *Fgf10* is also observed in mesenchyme immediately adjacent to lung buds (Bellusci et al., 1997b). At E12.5, control (Fig. 5C,E) and *Fgf9*$^{-/-}$ (Fig. 5D,F) lungs exhibited comparable expression of *Fgf10* in mesenchyme distal to budding airways.

At E13.5 (data not shown) and E14.5, *Fgf10* expression in *Fgf9*$^{-/-}$ (Fig. 5H,J) lungs was reduced relative to controls (Fig. 5G,I). In control E13.5-E14.5 lungs, mesenchymal foci of *Fgf10* expression were observed between most distal lung buds (arrowheads in Fig. 5I). Interbud mesenchyme in E13.5-E14.5 *Fgf9*$^{-/-}$ lungs often lacked *Fgf10* expression (arrowheads in Fig. 5J). Lung organ culture experiments have indicated that *Fgf10* expression in lateral interbud mesenchyme induces branching and outgrowth of new distal buds (Bellusci et al., 1997b). Hence, the lack of *Fgf10* in interbud mesenchyme in *Fgf9*$^{-/-}$ lungs may impair future branching of lung buds. In *Fgf9*$^{-/-}$ lungs, some buds that lacked adjacent *Fgf10* expression (arrow in Fig. 5H) were dilated with little surrounding mesenchyme. Similar premature bud dilation and mesenchymal hypoplasia were observed in E12.5 *Fgf9*$^{-/-}$ lungs (Fig. 1H). This suggests that reduced *Fgf10* expression in E13.5-E14.5 *Fgf9*$^{-/-}$ lungs may be secondary to a lack of mesenchyme. Dilation of airway buds in E12.5-E14.5 *Fgf9*$^{-/-}$ lungs and reduced *Fgf10* expression in E13.5-E14.5 *Fgf9*$^{-/-}$ lungs are both consistent with premature termination of airway branching in *Fgf9*$^{-/-}$ lungs.

DISCUSSION

In the embryonic lung, mesenchymally expressed *Fgf10* (Fig. 6A, top panel) and *Fgf7* have been previously shown to regulate epithelial development (Bellusci et al., 1997b). Here we show

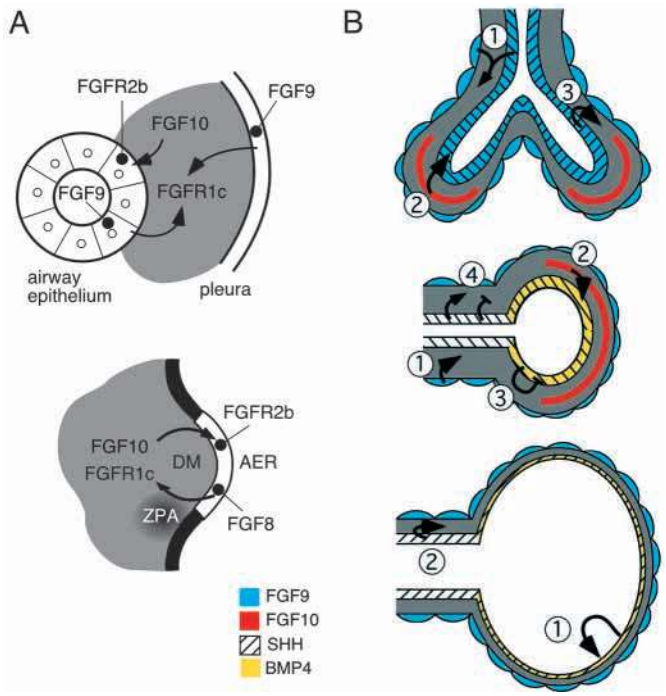

Fig. 6. Models for molecular signaling in developing lung. (A) Reciprocal FGF signaling between epithelium and mesenchyme during lung (top) and limb (bottom) embryogenesis. (A, top) We propose that FGF9 from the lung epithelium and pleura activates FGFR1c in the mesenchyme, while FGF10 from the mesenchyme activates FGFR2b in the epithelium. (A, bottom) Similar essential reciprocal epithelial-mesenchymal signaling between FGF10 in the mesenchyme and FGF8 in the overlying apical ectodermal ridge (AER) regulates limb bud outgrowth in mouse embryos. (DM, distal mesenchyme; ZPA, zone of polarizing activity). (FGF8 and FGF9 may also signal through FGFR2c, but *Fgfr1* is more highly expressed than *Fgfr2* in embryonic lung and limb mesenchyme (Peters et al., 1992).) (B) Model for interactions between Fgf and non-Fgf signaling pathways in developing lung. (B, top) Signaling during proximal airway branching in the early pseudoglandular period. (1) FGF9 (blue) in both airway epithelium and pleura stimulates mesenchymal proliferation. (Grey shading indicates mesenchyme.) (2) FGF10 (red) in the mesenchyme induces airway branching by stimulating endoderm proliferation and migration. (3) SHH (hatched) in the airway epithelium promotes mesenchymal proliferation. (B, middle) Signaling during airway branching in the late pseudoglandular period. (1) FGF9, now limited to the pleura, stimulates mesenchymal proliferation. (2) Mesenchymal FGF10 stimulates endoderm proliferation and migration, and appears to induce distal epithelial BMP4 expression (yellow). (3) BMP4 appears to inhibit airway branching by inhibiting endoderm proliferation, and perhaps by inhibiting endoderm migration. (4) SHH in the epithelium stimulates mesenchymal proliferation. Vascular defects in $Shh^{-/-}$ lungs indicate that *Shh* regulates development of mesenchymal vasculature. SHH also appears to prevent more generalized mesenchymal expression of *Fgf10* (truncated symbol). (B, bottom) Signaling during development of distal airspaces. Mesenchyme surrounding epithelial buds is sharply reduced; focally high *Fgf10* expression in the adjacent mesenchyme is lost; and epithelial differentiation begins with the narrowing of the epithelium. (1) Epithelial *Bmp4* expression is essential for distal epithelial differentiation. (2) Continued *Shh* expression in the epithelium may regulate vascular development. In this model, distal lung development proceeds when mesenchyme surrounding developing airways thins, *Fgf10* expression is reduced and *Bmp4* expression is high. In $Fgf9^{-/-}$ lungs, loss of *Fgf9*-induced mesenchymal proliferation could result in premature reduction in mesenchyme surrounding budding airways, leading to premature reduction in *Fgf10* expression. This would allow distal lung development to commence after fewer iterations of airway branching.

that an epithelial signal, FGF9, regulates lung mesenchymal development (Fig. 6A, top panel). While airway branching is reduced in $Fgf9^{-/-}$ lungs, it is completely absent in $Fgf10^{-/-}$ lungs (Min et al., 1998; Sekine et al., 1999). This suggests that FGF10 signaling initiates individual branch formation, whereas FGF9 signaling titrates the overall amount of branching in developing lung. FGF10, which is restricted to foci of high expression in mesenchyme, stimulates localized proliferation of adjacent epithelial cells (Bellusci et al., 1997b), and acts as a chemotactic factor for lung epithelial cells in vitro (Park et al., 1998). New lung buds apparently grow toward localized foci of high *Fgf10* expression (Fig. 6B, top). In contrast, *Fgf9* is expressed throughout lung epithelium and pleura at E10.5, and stimulates mesenchymal proliferation (Fig. 6B, top).

Mesenchymal regulation of airway branching

The reduced amount of mesenchyme in $Fgf9^{-/-}$ lungs suggests that *Fgf9* regulates airway branching by controlling mesenchymal expansion. Regulation of epithelial branching by lung mesenchyme is well documented (Hilfer, 1996; Hogan and Yingling, 1998). In fact, lung graft experiments have shown that the quantity of mesenchyme surrounding lung buds is proportional to the extent of branching observed (Masters, 1976). Also, as developing lung leaves the pseudoglandular phase (at about E16), the amount of mesenchyme decreases; concurrently, airway lumens dilate and the epithelial lining thins as differentiation of the epithelium progresses (Fig. 6B, bottom).

There are several mechanisms by which hypoplasia of lung mesenchyme could reduce airway branching. First, loss of mesenchyme could reduce *Fgf10* expression, thus removing the signal that instructs individual epithelial buds to branch. Reduced *Fgf10* expression in E13.5-E14.5 $Fgf9^{-/-}$ lungs is consistent with this hypothesis. Second, loss of mesenchyme in $Fgf9^{-/-}$ lungs could remove a signal that prevents premature epithelial differentiation during the pseudoglandular period. Investigation of this possibility will require detailed temporal studies of epithelial cell morphology and gene expression in $Fgf9^{-/-}$ versus control lungs. Finally, thick lung mesenchyme in the early embryo may mechanically inhibit dilation of distal epithelial buds. Thinning of mesenchyme in $Fgf9^{-/-}$ lungs would thus allow premature epithelial bud dilation by decreasing a physical constraint on epithelial expansion. Indeed, some epithelial buds in $Fgf9^{-/-}$ lungs appear to be dilating at E12.5-E13.5, whereas control lung buds are still branching. *Shh* mutant mice support the hypothesis that the amount of mesenchyme around budding airways affects airway dilation: lungs in which *Shh* is overexpressed using the surfactant C promoter show increased mesenchyme and reduced airway dilation (Bellusci et al., 1997a).

Complementary roles for *Fgf9* and *Fgf10* in lung development

Dynamic changes in foci of high *Fgf10* expression in the mesenchyme appear to stimulate epithelial branching early in

lung development (Bellusci et al., 1997b; Hogan and Yingling, 1998). Why airway branching stops is less well understood. *Fgf10* may contribute to the termination of branching by stimulating epithelial expression of the gene for bone morphogenetic protein 4 (*Bmp4*), which inhibits endoderm proliferation (Fig. 6B, middle) and is essential for distal lung differentiation (Fig. 6B, bottom) (Quaggin et al., 1999; Weaver et al., 2000; Weaver et al., 1999). Our results suggest a model in which *Fgf9* regulates the number of cycles of airway branching by regulating the amount of lung mesenchyme and the amount of mesenchymal *Fgf10* expression. Early in normal lung development, when *Fgf9* is expressed in both the epithelium and in the pleura, FGF9 signaling to mesenchyme is maximized, and proximal airway branching is prolific (Fig. 6B, top). After E12.5, when *Fgf9* is expressed only in the pleura, the amount of lung mesenchyme gradually decreases and airway branching subsequently slows (Fig. 6B, lower). *Fgf9*$^{-/-}$ lungs appear to 'run out' of mesenchyme prematurely, causing reduced airway branching. In this model, distal lung development occurs when mesenchyme surrounding developing airways decreases, *Fgf10* expression is decreased, and epithelial *Bmp4* expression is high (Fig. 6B, bottom). Normal lung lobe formation indicates that early airway branching proceeds normally in *Fgf9*$^{-/-}$ lungs, presumably occurring before the onset of critical mesenchymal depletion.

In vitro studies of mouse lung have shown that endoderm, but not the surrounding mesenchyme, migrates towards foci of *Fgf10* expression (Weaver et al., 2000). Unknown epithelial-mesenchymal interactions must occur to allow mesenchyme to continue to surround endoderm as it migrates (Weaver et al., 2000). Pleural *Fgf9* could mediate this process by stimulating mesenchymal proliferation and/or mesenchyme migration. In vitro studies have shown that exogenous FGF9 can stimulate cell migration into the developing ovary from neighboring mesonephric tissue (Colvin et al., 2001).

Preserved differentiation and morphology in *Fgf9*$^{-/-}$ lung

Development and differentiation of distal, respiratory airways may involve mechanical and molecular processes distinct from those regulating proximal lung development. Loss of epithelial *Bmp4* expression in *Pod1*$^{-/-}$ mice (Quaggin et al., 1999) and loss of BMP4 activity in mice expressing a dominant negative BMP receptor (Weaver et al., 1999) both result in failure of distal lung development. *Pod1*$^{-/-}$ lungs exhibit moderately reduced proximal airway branching, and a profound defect in terminal branching, showing no alveolar ducts, sacs or alveoli. In contrast, significant formation of distal airspaces and differentiation of Type I and Type II pneumocytes occur in *Fgf9*$^{-/-}$ lung, suggesting preserved *Bmp4* expression. Interestingly, *Fgf10* expression is not altered in *Pod1*$^{-/-}$ lung (Quaggin et al., 1999).

Reduced airway branching is observed in several knockout mice. *Fgf9*$^{-/-}$ mice are unique in that, other than reduced branching, they exhibit relatively normal lung morphology. Loss of BMP4 activity (Weaver et al., 1999), or loss of *Pod1* (Quaggin et al., 1999) or *Shh* (Pepicelli et al., 1998), each results in reduced branching with dysmorphic lung development. Our findings demonstrate that differentiation of proximal and distal lung epithelium and significant development of distal airways can occur in the absence of *Fgf9*. The small, but well-formed lungs in *Fgf9*$^{-/-}$ mice suggest that titration of *Fgf9* expression could effectively regulate lung size in vivo.

Analysis of male-to-female sex reversal in *Fgf9*$^{-/-}$ mice indicates that *Fgf9* also regulates growth of the embryonic testis, in part by stimulating mesenchymal proliferation (Colvin et al., 2001). As in developing *Fgf9*$^{-/-}$ lung, differentiation of all testicular cell types can occur without *Fgf9*. These results suggest that *Fgf9* regulates embryonic organ size in at least two systems by regulating mesenchymal expansion.

Epithelial-mesenchymal FGF signaling in lung and limb

Reciprocal signaling between epithelial and mesenchymal FGFs drives embryogenesis of multiple organs (Ohuchi et al., 2000). Epithelial tissues tend to express FGFRb splice forms, while mesenchymal tissues tend express FGFRc splice forms (Orr-Urtreger et al., 1993). FGF7 and FGF10 activate only the 'b' splice form of FGFR2 (FGFR2b) (Igarashi et al., 1998; Ornitz et al., 1996), while FGF9 preferentially activates FGFRc splice forms (Ornitz et al., 1996; Santos-Ocampo et al., 1996). Lungs of *Fgfr3/Fgfr4* double-null mice are histologically normal at birth (Weinstein et al., 1998), indicating that the lethal *Fgf10*$^{-/-}$ and *Fgf9*$^{-/-}$ lung phenotypes must involve decreased signaling through FGFR1 and/or FGFR2. These findings suggest that, in the developing lung, FGF10 and FGF7 signal from mesenchyme to epithelium through FGFR2b, while FGF9 signals from epithelium and pleura to mesenchyme, primarily through FGFR1c or FGFR2c (Fig. 6A, top). Similar epithelial-mesenchymal reciprocal signaling between FGF10 in mesenchyme and FGF4, FGF8, FGF9 and FGF17 in the overlying AER regulates embryonic mouse limb bud outgrowth (Lewandoski et al., 2000; Martin, 1998). Like *Fgf9* and *Fgf10* in lung, generation of null mutants has demonstrated that *Fgf8* and *Fgf10* are essential for limb embryogenesis (Fig. 6A, bottom; Lewandoski et al., 2000; Min et al., 1998; Sekine et al., 1999).

Overexpressing *Shh* in airway epithelium results in increased mesenchymal proliferation and increased mesenchymal tissue (Bellusci et al., 1997a), suggesting that FGF9 and hedgehog signaling may jointly regulate mesenchymal development in embryonic lung (Fig. 6B, top). Vascular defects in *Shh*$^{-/-}$ mice (Pepicelli et al., 1998), indicate that *Shh* may regulate development of mesenchymal vasculature. In the developing limb, *Shh* expression in the zone of polarizing activity (ZPA) is required to maintain *Fgf9* expression in the apical ectodermal ridge (AER; Sun et al., 2000; Fig. 6A, bottom). This finding, and normal *Shh* expression in *Fgf9*$^{-/-}$ lung, suggest that *Shh* may also act upstream of *Fgf9* during lung embryogenesis. Curiously, data from *Shh*$^{-/-}$ lungs (Pepicelli et al., 1998) and from transgenic lungs that overexpress *Shh* (Bellusci et al., 1997b) indicate that *Shh* negatively regulates *Fgf10* expression in developing lung (Fig. 6B, middle).

Fgf9 regulation of lung size and shape

Loss of functional thoracic cavity volume in utero, for example, because of diaphragmatic hernia, fetal pleural effusions or intrathoracic neoplasms, limits embryonic lung growth (Hasleton, 1996b). Our data indicate that *Fgf9*$^{-/-}$ lung

hypoplasia represents a primary defect in lung growth. No abdominal contents were ever found in the thoracic cavity of *Fgf9*$^{-/-}$ embryos, and *Fgf9*$^{-/-}$ mice could breathe and fill the lungs with air (data not shown), indicating that the diaphragm is intact and functional. Because *Fgf9* is expressed in the developing pleura, it is possible that malformation of the pleura could result in leakage of lung fluid into the thoracic cavity, constricting growth of thoracic organs. Selective loss of lung mesenchyme and the observation of cardiac dilation in some *Fgf9*$^{-/-}$ mice suggest otherwise. In addition, preservation of tight junctions between pleural cells and of the pleural basement membrane suggests that the barrier function of the pleura is retained in *Fgf9*$^{-/-}$ lungs. Normal vascular histology, vWF expression and capillary formation in *Fgf9*$^{-/-}$ lungs indicate that lung hypoplasia in *Fgf9*$^{-/-}$ mice is not secondary to gross vascular dysgenesis.

Fgf9$^{-/-}$ lungs fail to fill the thoracic cavity and lack the sharp contours of normal lungs, suggesting that *Fgf9* is an important regulator of lung size and shape. Pleural expression of *Fgf9* could potentially be altered by physical contact with structures surrounding the developing lung (such as the wall of the thoracic cavity in normal lung or intestine displaced into the thoracic cavity secondary to diaphragmatic hernia), allowing precise fitting of the developing lung into the available space. In support of this model, rat visceral pleural cells in vitro exhibit altered gene expression when subjected to fluid shear stress simulating the rubbing of the lung pleura against the chest wall (Waters et al., 1997).

Possible roles for *Fgf9* in carcinogenesis

Our data indicate that *Fgf9* stimulates fetal lung cell proliferation and regulates fetal lung size. These results suggest that exogenous FGF9 could potentially enhance human lung growth after surgical lung resection, a commonly used treatment for lung carcinoma. In addition, aberrant *Fgf9* upregulation could contribute to cancerous lung growth. Like prostate cancer, most lung carcinoma is epithelial in origin. During normal lung embryogenesis, epithelial *Fgf9* apparently stimulates mesenchymal proliferation by activating mesenchymal FGFRc splice forms. However, in vivo analysis of malignant transformation of prostate epithelial cells has demonstrated a switch from exclusive expression of FGFRb in epithelial cells to exclusive expression of FGFRc; upregulation of epithelial FGFs was also observed (Yan et al., 1993). In the lung, a similar upregulation of epithelial *Fgf9,* and aberrant expression of FGFRc splice forms in the epithelium, could create an autocrine loop driving pathologic epithelial proliferation.

In summary, we have demonstrated that *Fgf9* is essential for lung embryogenesis and for postnatal survival in mice, and we have identified a novel role for *Fgf9* in regulating lung mesenchyme. We provide evidence that *Fgf9* affects lung size by stimulating mesenchymal proliferation and mesenchymal *Fgf10* expression. Similar to *Fgf* function in other developmental systems, FGF9 signaling from the epithelium and reciprocal FGF10 signaling from the mesenchyme appear coordinately to regulate airway branching and lung growth in mouse embryos. As *Fgf9*$^{-/-}$ mice die at birth, study of these mice could not address *Fgf9* function in postnatal lung. Failure of alveogenesis in *Fgfr3/Fgfr4* double-null mice (Weinstein et al., 1998), and in vitro activation of FGFR3 and FGFR4 by FGF9 (Ornitz et al., 1996), suggest a possible role for *Fgf9* in alveogenesis, which occurs postnatally in mice.

We are grateful for technical assistance from E. Taylor, M. Scott, A. Johnson and B. Coleman (histology), E. Spinaio, X. Hua, L. Li, H. Walker and M. Wuerffel (animal husbandry), M. Veith (scanning electron microscopy), L. LaRose and M. Levy (transmission electron microscopy) and J. Waggoner (figure preparation). We thank B. Hogan for the *Fgf10* in situ probe, A. McMahon for the *Shh* in situ probe, J. Whitsett for the SP-C antibody and F. DeMayo for CCSP antibody. Our thanks to D. deMello and E. Crouch for helpful discussions, and to R. Pierce, S. Brody, R. Mecham and R. Cagan for review of the manuscript. This work was supported by grants from Monsanto/Searle and the American Heart Association (# 974-0221N).

REFERENCES

Bellusci, S., Furuta, Y., Rush, M. G., Henderson, R., Winnier, G. and Hogan, B. L. (1997a). Involvement of Sonic hedgehog (Shh) in mouse embryonic lung growth and morphogenesis. *Development* **124**, 53-63.

Bellusci, S., Grindley, J., Emoto, H., Itoh, N. and Hogan, B. L. (1997b). Fibroblast growth factor 10 (FGF10) and branching morphogenesis in the embryonic mouse lung. *Development* **124**, 4867-78.

Colvin, J. S., Feldman, B., Nadeau, J. H., Goldfarb, M. and Ornitz, D. M. (1999). Genomic organization and embryonic expression of the mouse fibroblast growth factor 9 gene. *Dev. Dyn.* **216**, 72-88.

Colvin, J. S., Green, R. P., Schmahl, J., Capel, B. and Ornitz, D. M. (2001). Male-to-female sex reversal in mice lacking fibroblast growth factor 9. *Cell* **104**, 875-889.

De Moerlooze, L., Spencer-Dene, B., Revest, J., Hajihosseini, M., Rosewell, I. and Dickson, C. (2000). An important role for the IIIb isoform of fibroblast growth factor receptor 2 (FGFR2) in mesenchymal-epithelial signalling during mouse organogenesis. *Development* **127**, 483-492.

deMello, D. E., Sawyer, D., Galvin, N. and Reid, L. M. (1997). Early fetal development of lung vasculature. *Am. J. Respir. Cell Mol. Biol.* **16**, 568-81.

Guo, L., Degenstein, L. and Fuchs, E. (1996). Keratinocyte growth factor is required for hair development but not for wound healing. *Genes Dev.* **10**, 165-175.

Hasleton, P. S. (1996a). Anatomy of the lung. In *Spenser's Pathology of the Lung* (ed. P. S. Hasleton), pp. 1-44. New York: McGraw-Hill.

Hasleton, P. S. (1996b). Embryology and development of the lung. In *Spenser's Pathology of the Lung* (ed. P. S. Hasleton), pp. 45-55. New York: McGraw-Hill.

Hilfer, S. R. (1996). Morphogenesis of the lung: control of embryonic and fetal branching. *Annu. Rev. Physiol.* **58**, 93-113.

Hogan, B. L. M. and Yingling, J. M. (1998). Epithelial/mesenchymal interactions and branching morphogenesis of the lung. *Curr. Opin. Genet. Dev.* **8**, 481-486.

Igarashi, M., Finch, P. W. and Aaronson, S. A. (1998). Characterization of recombinant human fibroblast growth factor (Fgf-10) reveals functional similarities with keratinocyte growth factor (Fgf-7). *J. Biol. Chem.* **273**, 13230-13235.

Kaartinen, V., Voncken, J. W., Shuler, C., Warburton, D., Bu, D., Heisterkamp, N. and Groffen, J. (1995). Abnormal lung development and cleft palate in mice lacking TGF-beta 3 indicates defects of epithelial-mesenchymal interaction. *Nat. Genet.* **11**, 415-421.

Kuzu, I., Bicknell, R., Harris, A. L., Jones, M., Gatter, K. C. and Mason, D. Y. (1992). Heterogeneity of vascular endothelial cells with relevance to diagnosis of vascular tumours. *J. Clin. Pathol.* **45**, 143-148.

Lewandoski, M., Sun, X. and Martin, G. R. (2000). Fgf8 signalling from the AER is essential for normal limb development. *Nat. Genet.* **26**, 460-463.

Martin, G. R. (1998). The roles of FGFs in the early development of vertebrate limbs. *Genes Dev.* **12**, 1571-1586.

Masters, J. R. (1976). Epithelial-mesenchymal interaction during lung development: the effect of mesenchymal mass. *Dev. Biol.* **51**, 98-108.

Min, H., Danilenko, D. M., Scully, S. A., Bolon, B., Ring, B. D., Tarpley, J. E., DeRose, M. and Simonet, W. S. (1998). Fgf-10 is required for both limb and lung development and exhibits striking functional similarity to *Drosophila* branchless. *Genes Dev.* **12**, 3156-3161.

Naski, M. C., Colvin, J. S., Coffin, J. D. and Ornitz, D. M. (1998). Repression of hedgehog signaling and BMP4 expression in growth plate

cartilage by fibroblast growth factor receptor 3. *Development* **125**, 4977-4988.

Ohuchi, H., Hori, Y., Yamasaki, M., Harada, H., Sekine, K., Kato, S. and Itoh, N. (2000). FGF10 acts as a major ligand for FGF receptor 2 IIIb in mouse multi-organ development. *Biochem. Biophys. Res. Commun.* **277**, 643-649.

Ornitz, D. M., Xu, J., Colvin, J. S., McEwen, D. G., MacArthur, C. A., Coulier, F., Gao, G. and Goldfarb, M. (1996). Receptor specificity of the fibroblast growth factor family. *J. Biol. Chem.* **271**, 15292-15297.

Ornitz, D. M. and Itoh, N. (2001). Fibroblast growth factors. *Genome Biol.* **2**, 3005.1-3005.12.

Orr-Urtreger, A., Bedford, M. T., Burakova, T., Arman, E., Zimmer, Y., Yayon, A., Givol, D. and Lonai, P. (1993). Developmental localization of the splicing alternatives of fibroblast growth factor receptor-2 (FGFR2). *Dev. Biol.* **158**, 475-486.

Park, W. Y., Miranda, B., Lebeche, D., Hashimoto, G. and Cardoso, W. V. (1998). FGF-10 is a chemotactic factor for distal epithelial buds during lung development. *Dev. Biol.* **201**, 125-34.

Pepicelli, C. V., Lewis, P. M. and McMahon, A. P. (1998). Sonic hedgehog regulates branching morphogenesis in the mammalian lung. *Curr. Biol.* **8**, 1083-1086.

Peters, K. G., Werner, S., Chen, G. and Williams, L. T. (1992). Two FGF receptor genes are differentially expressed in epithelial and mesenchymal tissues during limb formation and organogenesis in the mouse. *Development* **114**, 233-243.

Quaggin, S. E., Schwartz, L., Cui, S., Igarashi, P., Deimling, J., Post, M. and Rossant, J. (1999). The basic-helix-loop-helix protein pod1 is critically important for kidney and lung organogenesis. *Development* **126**, 5771-5783.

Ray, M. K., Wang, G., Barrish, J., Finegold, M. J. and DeMayo, F. J. (1996). Immunohistochemical localization of mouse Clara cell 10-KD protein using antibodies raised against the recombinant protein. *J. Histochem. Cytochem.* **44**, 919-927.

Santos-Ocampo, S., Colvin, J. S., Chellaiah, A. T. and Ornitz, D. M. (1996). Expression and biological activity of mouse fibroblast growth factor-9 (FGF-9). *J. Biol. Chem.* **271**, 1726-1731.

Sasaki, H. and Hogan, B. L. (1993). Differential expression of multiple fork head related genes during gastrulation and axial pattern formation in the mouse embryo. *Development* **118**, 47-59.

Satokata, I. and Maas, R. (1994). Msx1 deficient mice exhibit cleft palate and abnormalities of craniofacial and tooth development. *Nat. Genet.* **6**, 348-356.

Schor, A. M., Pazouki, S., Morris, J., Smither, R. L., Chandrachud, L. M. and Pendleton, N. (1998). Heterogeneity in microvascular density in lung tumours: comparison with normal bronchus. *Br. J. Cancer* **77**, 946-951.

Sekine, K., Ohuchi, H., Fujiwara, M., Yamasaki, M., Yoshizawa, T., Sato, T., Yagishita, N., Matsui, D., Koga, Y., Itoh, N. et al. (1999). Fgf10 is essential for limb and lung formation. *Nat. Genet.* **21**, 138-141.

Sun, X., Lewandoski, M., Meyers, E. N., Liu, Y. H., Maxson, R. E., Jr and Martin, G. R. (2000). Conditional inactivation of Fgf4 reveals complexity of signalling during limb bud development. *Nat. Genet.* **25**, 83-86.

Ten Have-Opbroek, A. A. (1981). The development of the lung in mammals: an analysis of concepts and findings. *Am. J. Anat.* **162**, 201-219.

Thurlebeck, W. M. (1995). Lung growth and development. In *Pathology of the Lung* (ed. W. M. Thurlebeck and A. M. Churg), pp. 37-87. New York: Theime Medical Publishers.

Waters, C. M., Chang, J. Y., Glucksberg, M. R., DePaola, N. and Grotberg, J. B. (1997). Mechanical forces alter growth factor release by pleural mesothelial cells. *Am. J. Physiol.* **272**, L552-L557.

Weaver, M., Yingling, J. M., Dunn, N. R., Bellusci, S. and Hogan, B. L. (1999). Bmp signaling regulates proximal-distal differentiation of endoderm in mouse lung development. *Development* **126**, 4005-4015.

Weaver, M., Dunn, N. R. and Hogan, B. L. (2000). Bmp4 and Fgf10 play opposing roles during lung bud morphogenesis. *Development* **127**, 2695-2704.

Weinstein, M., Xu, X., Ohyama, K. and Deng, C. X. (1998). FGFR-3 and FGFR-4 function cooperatively to direct alveogenesis in the murine lung. *Development* **125**, 3615-3623.

Wert, S. E., Glasser, S. W., Korfhagen, T. R. and Whitsett, J. A. (1993). Transcriptional elements from the human SP-C gene direct expression in the primordial respiratory epithelium of transgenic mice. *Dev. Biol.* **156**, 426-443.

Yan, G., Fukabori, Y., McBride, G., Nikolaropolous, S. and McKeehan, W. L. (1993). Exon switching and activation of stromal and embryonic fibroblast growth factor (FGF)-FGF receptor genes in prostate epithelial cells accompany stromal independence and malignancy. *Mol. Cell. Biol.* **13**, 4513-4522.

Zhou, L., Lim, L., Costa, R. H. and Whitsett, J. A. (1996). Thyroid transcription factor-1, hepatocyte nuclear factor-3beta, surfactant protein B, C, and Clara cell secretory protein in developing mouse lung. *J. Histochem. Cytochem.* **44**, 1183-1193.